The energy distribution of β CrB for the specific stellar abundances

F. Castelli

CNR-Gruppo Nazionale Astronomia and Osservatorio Astronomico di Trieste

Abstract. The comparison of the observed and computed energy distributions of β CrB has shown that a model with the specific chemical composition of the star can account for the visual enery distribution, while it is still unable to reproduce ultraviolet observations shortward of 1700 Å. Furthermore, the predicted absorption of strong Fe II and Mg II UV lines is much larger than the observed one.

Key words: Stars: chemically peculiar - Stars: energy distribution

1. Introduction

Some magnetic Ap stars, as β CrB (HD 137909, HR 5747, F0p) and 33 Lib (HD 137949) show an excess of ultraviolet flux shortward of 2000 Å when compared both with other peculiar or normal stars of similar spectral type (i.e. 60 Tau = HD 27628, 78 Tau = HD 28319) and with energy distributions computed for solar or solar scaled abundances.

Hack et al. (1997) explained the UV excess of β CrB ($T_{\rm eff}$ = 7950 K, $\log g$ = 4.3 from their paper) as due to a λ Boo companion having [M/H]=-1.0 and $T_{\rm eff}$ equal to about 8200 K. However, the hypothesis of a silicon deficiency which increases the ultraviolet flux was also suggested.

In this paper, we show that models computed with approximate specific abundances of β CrB explain the observed depressions at 4200 Å and 5200 Å, but are not able to explain the observed UV excess.

2. The far UV continous absorptions

Figure 1 shows that the energy distribution of stars with $T_{\rm eff}$ = 8000 K and $\log g$ = 4.0 is dominated shortward of 1700 Å by the discontinuities of C I (1240 Å; 1445 Å) and of Si I (1520 Å ; 1677 Å). The red wing of Ly$_\alpha$ yields also an important contribution up to about 1450 Å in stars with solar metallicity, but its effect on the observed flux decreases with increasing metallicity.

Therefore, when the energy distribution is computed, correct values for the carbon and silicon abundances should be used. While the ATLAS9 code (Kurucz, 1993) does not permit to change the abundances in an arbitrary way, owing to the pretabulated ODF's functions, arbitrary abundances can be used in the

Contrib. Astron. Obs. Skalnaté Pleso **27**, (1998), 192– 196.

ATLAS12 code (Kurucz, 1996), which computes line blanketing by means of the opacity sampling method.

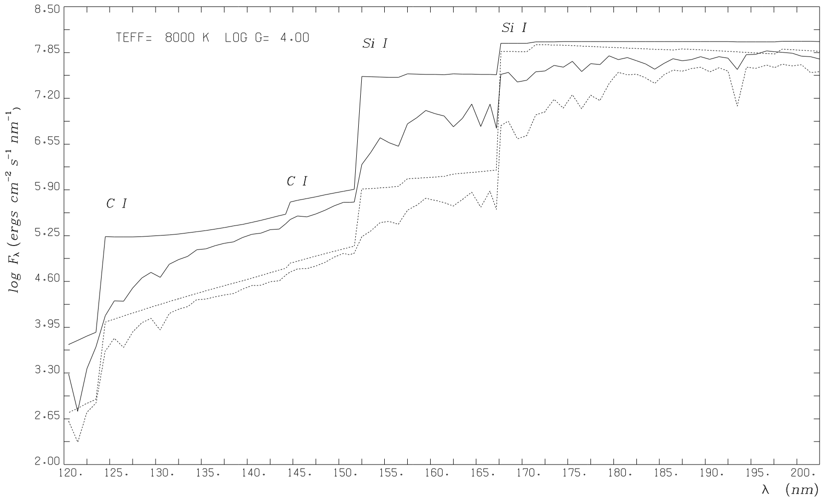

Figure 1. Comparison of fluxes from models having the same parameters $T_{\rm eff}$ = 8500 K and $\log g = 4.0$ and different metallicities [M/H]=0.0 (full line), and [M/H]=+1.0 (dotted line). The continous absorption is also plotted for each model

3. The computed energy distribution for specific abundances

To derive the energy distribution for the specific abundances of β CrB, we performed the following steps:

1) By comparing the dereddened observed c and (b-y) indices with the computed ones we derived the model parameters $T_{\rm eff} = 7950$ K, $\log g = 4.3$, and by comparing the observed and computed magnitudes (relative to 5556 Å) in the Balmer jump region we derived [M/H]=-1.0. Observed spectrophotometry was taken from Pyper & Adelman (1985).

2) We compared observed and computed high-resolution spectra in the visible region. The abundances and the microturbulent velocity were modified to fit the largest number of observed features. Spectroscopic observations cover the ranges 4130-4544 Å at 20000 resolution, 6076-6163 Å and 6629-6720 Å at 45000 resolution. They were taken at Haute-Provence Observatory by R. Faraggiana and at Crimean Astrophysical Observatory by N. Polosukhina. The synthetic spectra were computed by using the SYNTHE code (Kurucz, 1993) and the atomic line data from Kurucz (1995). The abundances listed in Table 1 correspond to a microturbulent velocity $\xi = 0\ \mathrm{km\,s^{-1}}$. While the spectra are better fitted by $\xi = 2\ \mathrm{km\,s^{-1}}$ for $\lambda > 6000$ Å , the zero value yields very strong computed features in the 4300 Å region. Because most of the lines are so weak for

Table 1. The abundances $\log(N_{\rm elem}/N_{\rm tot})$ for β CrB for $T_{\rm eff}$ = 7950 K, $\log g$ = 4.3, [M/H]=-1.0 and $\xi = 0$ km s^{-1}

	Elem	Sun	β CrB	[M/H]		Elem	Sun	β CrB	[M/H]
3	Li	-10.88	-8.28	[+2.60]	25	Mn	−6.65	-5.65	[+1.00]
6	C	-3.48	-3.98	[−0.50]	26	Fe	−4.53	-3.27	[+1.26]
7	N	-3.99	-3.99	[+0.00]	27	Co	−7.12	-6.12	[+1.00]
8	O	-3.11	-4.00	[−0.89]	28	Ni	−5.79	-5.69	[+0.00]
11	Na	-5.71	-5.71	[+0.00]	31	Ga	−9.16	-7.66	[+1.50]
12	Mg	-4.46	-4.46	[+0.00]	56	Ba	−9.91	-7.91	[+2.00]
13	Al	-5.57	-6.77	[−1.20]	57	La	−10.82	-8.17	[+2.65]
14	Si	-4.49	-4.49	[+0.00]	58	Ce	−10.49	-7.09	[+3.40]
20	Ca	-5.68	-5.00	[+0.68]	62	Sm	−11.04	-9.04	[+2.00]
21	Sc	-8.94	-7.94	[+1.00]	63	Eu	−11.53	-6.63	[+4.90]
22	Ti	-7.05	-6.05	[+1.00]	64	Gd	−10.92	-7.02	[+3.90]
23	V	-8.04	-7.04	[+1.00]	70	Yb	−10.96	-8.96	[+2.00]
24	Cr	-6.37	-4.67	[+1.70]					

$\lambda >$ 6000 Å that the differences between spectra computed with different ξ values are not very large, we preferred to adopt a zero value for ξ. Very probably the inconsistency between the line strengths at 4300 Å and 6000 Å would be removed with the inclusion of the magnetic field effects in the synthetic spectrum.

Table 1 shows that the estimated abundances of β CrB are very different from solar scaled abundances. In fact, the iron abundance is 10 times the solar one, but the silicon abundance is solar, and the carbon abundance is less than solar. Finally, the abundances of the heavy elements are enhanced much more than 10 times over the solar ones.

3) By using the abundances listed in Table 1 we computed an ATLAS12 model and a whole synthetic spectrum at 500000 resolution for the range 900-8000 Å. Then, we degraded the computed spectrum at the ODF's resolution, at 3 Å resolution, and at 1 Å resolution, in order to compare it with the ATLAS9 energy distribution and with IUE observations.

4. Results

Figure 2 shows that the new computed energy distribution reproduces very well the depressions observed at 4200 Å, and rather well that observed at 5200 Å. Our computations indicate that these depressions are due to the very large number of lines of heavy elements observed in these regions, in particular Ce and Gd.

Figure 3 compares the observed and computed energy distributions in the ultraviolet region. The data of the IUE image SWP44998 (dashed line) well correspond to the observations taken from the TD1 S2/68 Catalogue (Jamar et al.,

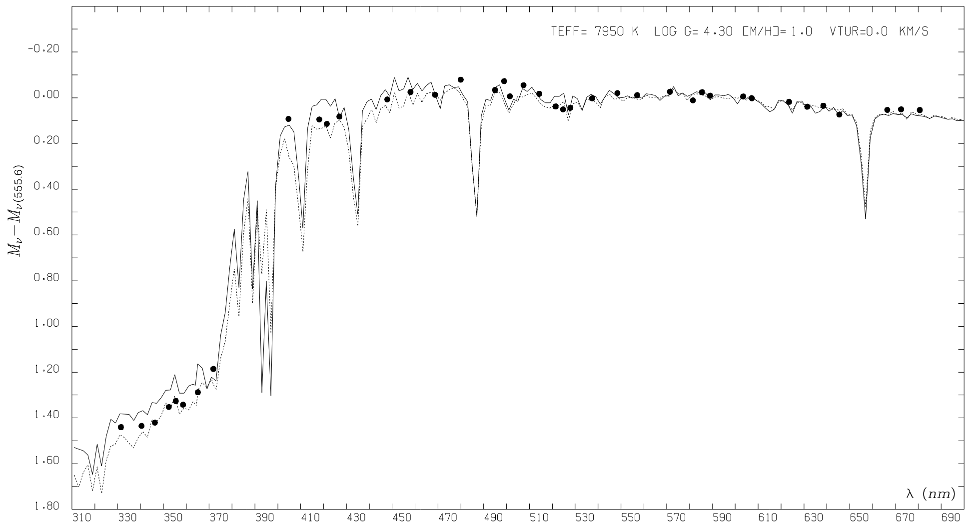

Figure 2. The visible energy distributions (in mag, relative to 5556 Å) from both ATLAS9 (full line) and ATLAS12 (dotted line) models are compared with the observations (dark points).

1976) (points). The excess of observed ultraviolet flux con not be predicted by a model computed with the specific abundances of the star. Also the computed strong blanketing at 2300 Å is not observed. The analysis of the high-resolution IUE image LWR07000 has shown that all the strong Fe II lines of the UV multiplets 2 and 3 are much weaker than the predicted ones. The discrepancy is not removed even by assuming solar iron abundance for β CrB. This behaviour is common to all the strong ultraviolet lines, including the Mg II lines at 2800 Å. Babel (1994) observed a similar disagreement for the Ca II resonance lines and he explained it with abundance stratifications.

5. Conclusions

An atmospheric model computed for the specific abundances of β CrB is still unable to reproduce the ultraviolet observations, which show an excess of ultraviolet flux shortward of 1700 Å and show profiles of the strong Fe II and Mg II lines much weaker than the predicted ones.

Therefore, either the ATLAS12 model can still not predict the spectrum of β CrB, owing to the lack, in the code, of treatment of magnetic field effects and inhomogeneous chemical distributions, or we actually observe the combined fluxes of β CrB and of the unknown companion, which could well be a λ Boo star, but also a much cooler star affected by chromospheric emissions.

33 Lib shows a similar behaviour, but we have not been able as yet to extend the sample to more stars, owing to a dramatic lack of IUE low resolution observations of Ap stars.

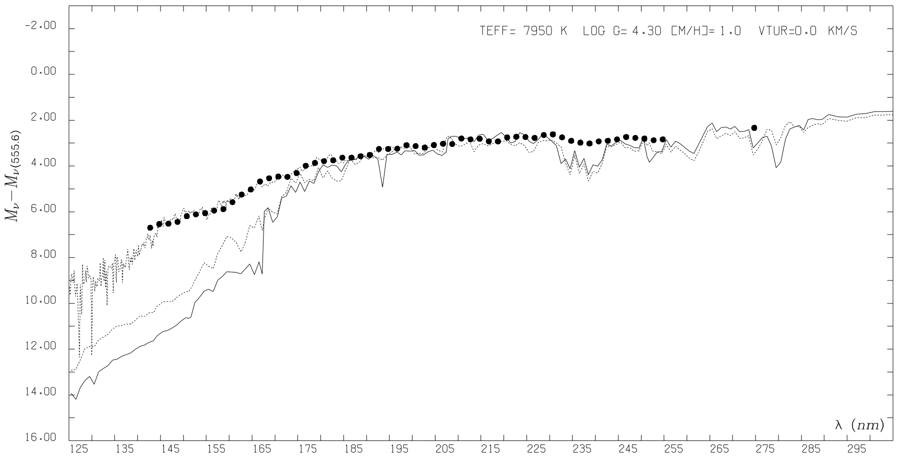

Figure 3. The ultraviolet energy distributions (in mag, relative to 5556 Å) from both ATLAS9 (full line) and ATLAS12 (dotted line) models are compared with the IUE (dashed line) and TD1 S2/68 (dark points) observations

References

Babel, J.: 1994, *Astron. Astrophys.* **283**, 189

Hack, M., Polosukhina, N.S., Malanushenko, V.P., Castelli, F.: 1997, *Astron. Astrophys.* **319**, 637

Jamar, C., Macau-Hercot, D., Monfils, A., Thompson, G.I., Houziaux, L., Wilson, R.: 1976, *Ultraviolet Bright-Star Spectrophotometric Catalogue*, ESA SR-27

Kurucz, R.L.: 1993, *ATLAS9 Stellar Atmosphere Programs and 2 km/s grid*, CD-ROM No 13

Kurucz, R.L.: 1993, *SYNTHE Spectrum Synthesis Programs and Line Data*, CD-ROM No 18

Kurucz, R.L.: 1995, *Atomic Line List*, CD-ROM No 23

Kurucz, R.L.: 1996, in *Stellar Surface Structure*, eds.: K.G. Strassmeier and J.L. Linsky, IAU Symp., 176, 523

Pyper, D.M., Adelman, S.J.: 1985, *Astron. Astrophys., Suppl. Ser.* **59**, 369